Available online at www.sciencedirect.com
ScienceDirect
International Journal of Thermal Sciences 47 (2008) 1069–1076
International Journal of Thermal Sciences
www.elsevier.com/locate/ijts

Critical flashing flow in convergent–divergent nozzles with initially subcooled liquid

Jinghui Liu *, Jiangping Chen, Zhijiu Chen

School of Mechanical Engineering, Shanghai Jiaotong University, Shanghai 200240, China

Received 13 January 2007; received in revised form 16 May 2007; accepted 27 July 2007

Available online 29 August 2007

Abstract

Investigation on critical flashing flow of initially subcooled water in convergent–divergent nozzles is carried out in this paper. A two-dimensional axial symmetric model is developed. In this model, the explosive flashing process immediately downstream the throat is modeled as an oblique evaporation wave, and the velocity direction change of the supersonic flow downstream the oblique evaporation wave is regarded to be resulted by an oblique shock wave. The further fluid expansion in the divergent section is assumed to be in Isentropic Homogeneous Equilibrium (IHE) except near the throat. The results show that the pressure immediately downstream the throat predicted by Abuaf's model is very close to the experimental result, about 4% deviation from Akagawa's tested value. Non-homogeneous equilibrium region exists downstream the oblique evaporation wave near the throat in the divergent section. The length of the non-homogeneous equilibrium region is increased as the inlet subcooled degree is increased. The pressure profile predicted by the model agrees very well with the tested profile of Akagawa except in the non-homogeneous equilibrium region near the throat.

Keywords: Convergent–divergent nozzle; Critical flow; Evaporation wave; Flashing flow; Metastable liquid

1. Introduction

In many situations, a pressurized liquid may rapidly expand into a low pressure environment. For example, refrigerants flowing through expansion devices (such as valve, capillary, short tube, nozzle, etc.) in refrigeration systems and disastrous industrial rupturing accidents of pressurized liquefied gas storage tank. If the low environmental pressure is low enough, the liquid will undergo a fast phase transition process and the mass flow rate will not be increased with the decreasing back pressure any more, i.e. the critical flashing flow.

The critical mass flow rate is the most important character of the critical flashing flow. The investigation results of Thompson et al. [1,2] have revealed that because of the different wave propagating speeds of liquid and two-phase mixture, rapid adiabatic expansion of liquid may produce a superheated metastable state and will make the evaporation discontinuity. Many other investigations [3–11] have also found the phenomenon. Several reviews of the literature pertaining to critical discharge of flashing flows, including those by Hutmacher [12], Hsu [13], Saha [14], and Isbin [15], have generally found that models based on assumptions of Isentropic Homogeneous Equilibrium (IHE) under-predict the critical discharge rate. The differences are attributed to the presence of non-equilibrium resulting in the superheated liquid. In order to evaluate this effect, Alamgir et al. [3] investigated the rapid blowdown depressurized hot water and suggested a semi-empirical formula to predict the pressure undershoot (or the liquid superheated degree) before flashing occurrence. On the basis of Alamgir et al., Jones [4] suggested an equation to predict the pressure undershoot at the throat of convergent–divergent nozzles. Further, Abuaf et al. [5] improved Jones's method and suggested a unified theory for the calculation of critical mass flux, whose accuracy is within 5%.

Sometimes, researchers are very interested to know how the pressure of the critical flashing flow is distributed along the flow direction, especially in what state the fluid is at the exit. In order get the purpose, the models of bubble formation and growth are needed. On the basis of the mass, momentum, and energy con-

* Corresponding author. Tel.: +086 02134206585; fax: +086 02134206814.
E-mail address: liujinghui@sjtu.edu.cn (J. Liu).

1290-0729/$ – see front matter
doi:10.1016/j.ijthermalsci.2007.07.019

servation laws, Elias and Chambre [16], Richter [17], Ardron [18], Shin and Jones [19], and Blinkov et al. [20] respectively established different two-phase fluid models to investigate the critical flow in nozzles or pipes. Pinhasi [21] gave a detailed review of the modeling of flashing two-phase flow. These models are all based on the step proceeding method. The selection of the bubble growth and formation models will distinctively influence the results.

Since flashing is delayed when initially subcooled liquid rapidly expands, where is the flashing inception (the intense nucleation point) located? Schrock et al. [6] investigated the flashing inception point of initially subcooled water in convergent–divergent nozzles, and found that the flashing inception point is located immediately upstream the throat and nearly has nothing to do with the initially inlet subcooled degree. Abuaf et al. [5] suggested that the flashing inception is located at the minimal area plane (throat) of the convergent–divergent nozzle when the flow is stable. Although there are evidences that the bubbles are created in front of the nozzle throat [16–19], the result of Shin and Jones [19] shows that the computed maximum throat void fraction is less than 1%, which supports Abuaf's result [5]. On the basis of this fact, Schrock et al. [6] suggested a two-step model to investigate the pressure profile in the convergent–divergent nozzles, and found that it only could give the pressure profile in the divergent section with trend and magnitudes similar to the tested data.

Superheated liquid will explosively evaporate in a narrow and observable region, i.e. evaporation wave [7–9]. Simoes-Moreira [9] established the evaporation wave theories (normal evaporation wave theory and oblique evaporation wave theory) and gave the choking condition for the normal evaporation wave. Employing the normal evaporation wave theory, he investigated the highly expanded flashing liquid jets [10] and explained the pressure drop and flashing mechanism in refrigerant expansion devices [11]. Simoes-Moreira [10,11] got the critical mass flux through experiments and regarded the explosive evaporation process as a normal evaporation wave which takes the shape of an equivalent hemisphere. He did not suggest how to calculate the critical mass flux and the liquid superheated degree immediately upstream the evaporation wave for the given inlet stagnation conditions. Documentaries [9–11] of the evaporation of liquid jet discharging into a low pressure environment using short-duration photographic techniques have revealed that the liquid core in the evaporation wave process takes the shape of a cone, and the velocities immediately upstream and downstream the evaporation wave are not normal to the evaporation surface. On the basis of this fact, Simoes-Moreira [9] established the oblique evaporation wave theory. In his oblique evaporation wave theory, he introduced three properties of the oblique evaporation wave similar to a regular compression shock wave, which are: (1) the relative velocities are coplanar with the vectors normal to the wave front, (2) the tangential velocity component is invariant across the wave, (3) the stagnation specific enthalpy is invariant in a stationary oblique evaporation wave. He also investigated the relationship between the velocity turning angle and the evaporation wave angle. But the superheated degree upstream the evaporation wave, which he did not suggest how to calculate for the given inlet stagnation conditions, must be known beforehand in the characteristics calculation of the oblique evaporation waves.

In this paper, in order to investigate the pressure distribution along the flow direction in a convergent–divergent nozzle and the fluid state at the nozzle exit, the authors assumed the maximal mass flux normal to the evaporation wave surface is the choked condition for flashing flow. Employing the oblique evaporation wave theory of Simoes-Moreira, the behaviors of initially subcooled liquid flashing flow in the convergent–divergent nozzles are investigated.

2. Model description

2.1. Oblique evaporation wave in convergent–divergent nozzles

As stated in introduction, the initially subcooled liquid is accelerated in the convergent section of the nozzle, and owing to the flashing delay, it becomes superheated at the throat. Then abrupt evaporation occurs immediately downstream the throat, and the superheated liquid begins to be turned into two-phase mixture. The liquid core takes the shape of a cone and will maintain for a distance downstream before disappearing. The velocity of the two-phase mixture immediately downstream the oblique evaporation wave is supersonic. The fluid behaviors are shown in Fig. 1.

In order to solve evaporation wave's parameters, some hypotheses are made as the following.

- The flow is stable. The flashing inception point (intense nucleation point) is located at the throat.
- The pressure in liquid core downstream the throat is constant, which is equal to the pressure at the flashing inception point.
- The velocity direction of the liquid core is along the flow axis.
- The thickness of the evaporation wave is neglected.
- The fluid immediately downstream the evaporation wave is in mechanical and homogeneous equilibrium.

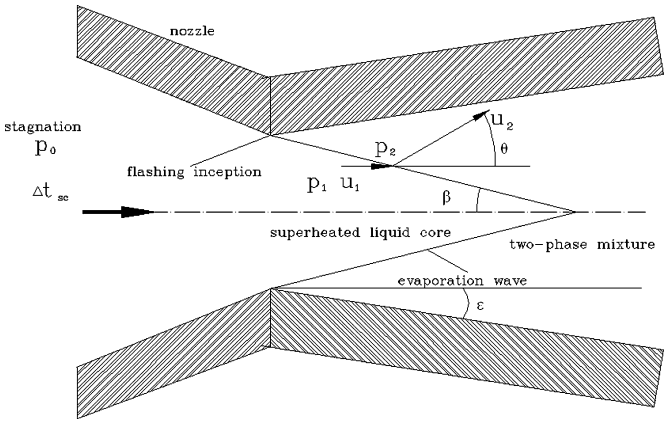

Fig. 1. Diagram of oblique evaporation wave in convergent–divergent nozzles.

- The choked condition for flashing flow is the superficial mass flux normal to the oblique evaporation wave surface gets the maximum, i.e. $dJ^2 = 0$.

According to the properties of oblique evaporation wave given by Simoes-Moreira [9], the laws of conservation of mass, momentum, and energy can be respectively written as

$$\frac{u_1}{v_1}\sin\beta = \frac{u_2}{v_2}\sin(\beta+\theta) \tag{1}$$

$$p_1 + \frac{u_1^2}{v_1}\sin^2\beta = p_2 + \frac{u_2^2}{v_2}\sin^2(\beta+\theta) \tag{2}$$

$$h_0 = h_2 + 0.5u_2^2 \tag{3}$$

where, u is velocity (m/s), v is specific volume (m^3/kg), β is evaporation wave angle, θ is velocity turning angle, p is pressure (Pa), h is enthalpy (J/kg). The subscripts 0, 1, 2 represent the inlet stagnation condition, the state immediately upstream the evaporation wave, and the state immediately downstream the evaporation wave respectively.

The tangential velocity component is invariant across the evaporation wave (Simoes-Moreira [9]). One can obtain the relationship between the velocities immediately upstream and downstream the evaporation wave.

$$u_1\cos\beta = u_2\cos(\beta+\theta) \tag{4}$$

As shown in Fig. 1, the superficial mass flux normal to the evaporation surface can be expressed as

$$J = \frac{u_1\sin\beta}{v_1} = \frac{u_2\sin(\beta+\theta)}{v_2} \tag{5}$$

Combining Eqs. (2) and (5), one can obtain the following equation analogous to that of normal evaporation waves [9].

$$J^2 = -\frac{p_2 - p_1}{v_2 - v_1} \tag{6}$$

The mathematical statement of maximal superficial mass flux is given by $dJ^2 = 0$, under which the normal component of the velocity immediately downstream the evaporation wave reaches sonic. For a given upstream state 1, the condition of the maximum mass flux applied to Eq. (6) results in

$$\frac{dv_2}{dT_2} = -\frac{1}{J_{C\text{–}J}^2}\frac{dp_2}{dT_2} \tag{7}$$

where, $J_{C\text{–}J}$ is the superficial mass flux normal to the evaporation wave surface at the Chapman–Jouguet (C–J) point in the p–v diagram.

The state 1 immediately upstream the evaporation wave is unknown. For the given stagnation conditions at the nozzle entrance, in order to calculate the critical mass flux and the oblique evaporation wave parameters, the relationship between the stagnation condition and the state immediate upstream the evaporation wave must be established. From the first hypothesis in Section 2.1, it can be deduced that the flashing flows with a subcooled inlet condition is single-phase liquid flow upstream of the throat. From the Bernoulli equation for single phase incompressible fluid, one can have the following equation.

$$p_0 - p_1 = \frac{u_1^2}{2C_D^2 v_1} \tag{8}$$

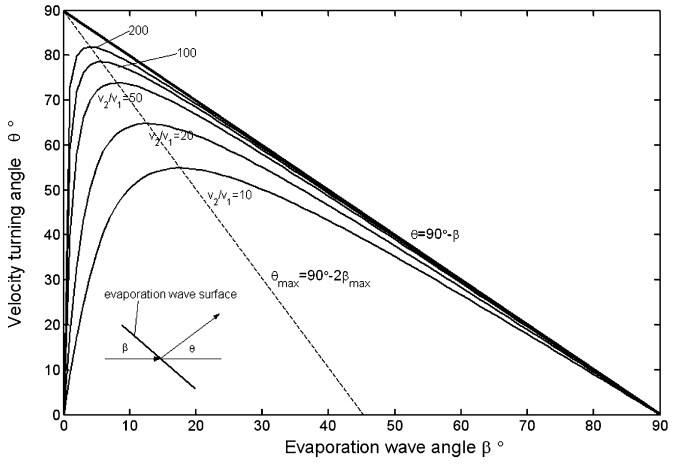

Fig. 2. The velocity turning angle θ as a function of the evaporation wave angle β for several specific volume ratios.

where, C_D is mass flow rate coefficient which is constant for incompressible single-phase flow.

Combining Eqs. (1) and (4), the following relationship between β and θ exists.

$$\tan\theta = \frac{\sin\beta\cos\beta}{\sin^2\beta + \frac{1}{v_2/v_1 - 1}} \tag{9}$$

In the evaporation wave angle range between 0° and 90° and knowing that the two-phase specific volume is necessarily higher than the superheated liquid specific volume, that is, $v_2/v_1 > 1$, the velocity turning angle θ has the same sign as the evaporation wave angle β. The relationship is shown in Fig. 2.

The extreme conditions can be obtained by differentiating Eq. (8) with respect to β and setting it to zero. J.R. Simoes-Moreira [9] gave their relationship as the following.

$$\theta_{\max} = \frac{\pi}{2} - 2\beta_{\max} \tag{10}$$

2.2. The liquid superheated degree upstream the oblique evaporation wave

Eqs. (1)–(4), (7) and (8) have 7 variables which are p_1, u_1, p_2, u_2, x_2, β, θ respectively. In order to solve the model, another equation must be found. In the introduction, one knows that Abuaf's model can precisely predict the superheated degree at the throat. Therefore, one can employ Abuaf's model to predict the pressure (p_1) upstream the evaporation wave. Then Eqs. (1)–(4), (7) and (8) can be solved.

According to Abuaf's model [5], the pressure undershoot at the flashing inception can be calculated by the following equation.

$$\Delta p_{Fi}^* = \frac{\Delta p_{Fi}}{\Delta p_{Fio}} = \text{Max}\begin{cases} 0 \\ 1 - 27\left[\dfrac{\bar{u}'^2}{u_0^2}\right]\left[\dfrac{A}{A_0}\right]^n F_i \end{cases} \tag{11a}$$

where

$$n = \begin{cases} 1.75, & A/A_0 \geqslant 1/6 \\ 1.4 & A/A_0 < 1/6 \end{cases} \tag{11b}$$

where, A is flow area (m^2); ΔP_{Fi} is pressure undershoot at flashing inception (Pa); ρ is density (m^3/kg).

The flashing index is defined as $F_i = \rho_l u^2/2\Delta p_{Fio}$. The turbulent intensity $\sqrt{u'^2}/u_0$ can be assumed to be 0.072. The static compression effects Δp_{Fio} can be calculated by Alamgir and Lienhar's model.

$$\Delta p_{Fio} = p_s - p_{Fi} = 0.253\frac{\sigma^{1.5}}{\sqrt{kT_c}}\frac{T_r^{13.73}\sqrt{1+14\Sigma^{0.8}}}{\left(1-\frac{v_l}{v_g}\right)} \tag{12}$$

where, p_s and p_{Fi} are the saturated pressure and the pressure at the flashing inception respectively; σ is surface intension; k is Boltzmann constant; T_c and T_r are the critical temperature and the reduced initial temperature respectively; The subscripts l and g represent the saturated liquid and the saturated vapor respectively.

For stable flow, Abuaf [5] suggested that the static depressurization rate can be calculated by the following equation.

$$\Sigma = \frac{J_c^3}{\rho_l^2}\cdot\frac{\mathrm{d}[\ln(A)]}{\mathrm{d}z} \tag{13}$$

Since the flashing inception is located at the throat, the fluid between the entrance and the throat is single phase fluid. The mass flux can be calculated by Bernoulli equation. The critical mass flux at the throat is given by

$$J_c = C_D\sqrt{2\rho_l(p_0 - p_s + \Delta p_{Fi})} \tag{14}$$

The pressure at the flashing inception can be calculated by

$$p_1 = p_s - \Delta p_{Fi} \tag{15}$$

2.3. Oblique evaporation wave model solution method

Because the pressure upstream the evaporation wave p_1 can be predicted by Abuaf's model, Eqs. (1)–(4), (7) and (8) have six variables, which are u_1, p_2, u_2, x_2, β, θ respectively. The oblique evaporation wave can be solved.

From Fig. 1, the relationship between the critical mass flux at the throat and the critical mass flux normal to the evaporation wave surface can be given by

$$J_{\mathrm{C\text{–}J}} = J_c\sin\beta \tag{16}$$

It can be incorporated into Eqs. (2), (3) and (7)

$$p_1 + v_1 J_c^2\sin^2\beta = p_2 + v_2 J_c^2\sin^2\beta \tag{17}$$

$$h_0 = h_2 + \frac{v_2^2 J_c^2\sin^2\beta}{2\sin^2(\beta+\theta)} \tag{18}$$

$$\frac{\mathrm{d}v_2}{\mathrm{d}T_2} = -\frac{1}{J_c^2\sin^2\beta}\frac{\mathrm{d}p_2}{\mathrm{d}T_2} \tag{19}$$

Combining Eqs. (9), (18) and (19), one can obtain

$$\tan^2\beta = \frac{2(h_0-h_2) - J_1^2 v_1^2}{J_1^2 v_2^2 - 2(h_0-h_2)} \tag{20}$$

Eq. (20) can be incorporated into Eq. (17)

$$p_1 - p_2 = \frac{2(h_0-h_2) - J_1^2 v_1^2}{(v_2+v_1)} \tag{21}$$

From Eq. (21), one can obtain

$$x_2 = \frac{2(h_0-h_{l2}) + (v_{l2}+v_1)(p_2-p_1) - J_1^2 v_1^2}{2(h_{g2}-h_{l2}) - (v_{g2}-v_{l2})(p_2-p_1)} \tag{22}$$

Combining Eqs. (19) and (20), one can obtain

$$\frac{\mathrm{d}v_2}{\mathrm{d}T_2} = -\frac{v_2^2 - v_1^2}{2(h_0-h_2) - J_1^2 v_1^2}\frac{\mathrm{d}p_2}{\mathrm{d}T_2} \tag{23}$$

Eqs. (22) and (23) only have two variables which are p_2 and x_2 respectively. They can be solved with iteration method.

2.4. Oblique shock wave in divergent section

Owing to the velocity turning angle downstream the oblique evaporation wave is usually not equal to the half of the nozzle divergent angle, the flow direction must be changed in the divergent section because of the restriction of the nozzle wall. From the knowledge of the compressible fluid dynamics, shock wave must occur when supersonic flow changes its direction by flowing through a concave surface. The behaviors of the fluid downstream the evaporation wave are depicted in Fig. 3.

According to the oblique shock wave theory, the following equations can be listed.

$$u_2\cos\omega = u_3\cos(\omega-\alpha) \tag{24}$$

$$\frac{u_2\sin\omega}{v_2} = \frac{u_3\sin(\omega-\alpha)}{v_3} \tag{25}$$

$$p_2 + \frac{u_2^2\sin^2\omega}{v_2} = p_3 + \frac{u_3^2\sin^2(\omega-\alpha)}{v_3} \tag{26}$$

$$h_0 = h_3 + \frac{1}{2}u_3^2 \tag{27}$$

where, ω and α are the shock wave angle and the velocity turning angle downstream the shock wave respectively; The subscript 3 represents the state immediately downstream the shock wave.

Eqs. (24)–(27) have five variables which are p_3, x_3, u_3, α, ω respectively. In order to solve the shock wave, another equation should be found.

Combining Eqs. (26) and (27), one can obtain the relationship between the shock wave angle ω and the velocity turning angle α. The relationship is shown in Fig. 4.

$$\tan\alpha = \frac{(v_2-v_3)\,\mathrm{tg}\,\omega}{v_2 + v_3\,\mathrm{tg}^2\,\omega} \tag{28}$$

Shown as in Fig. 4, similar to the oblique evaporation wave, there is a maximum for the velocity turning angle. If the angle between the velocity downstream the evaporation wave (u_2) and the nozzle wall is bigger than the maximal turning angle,

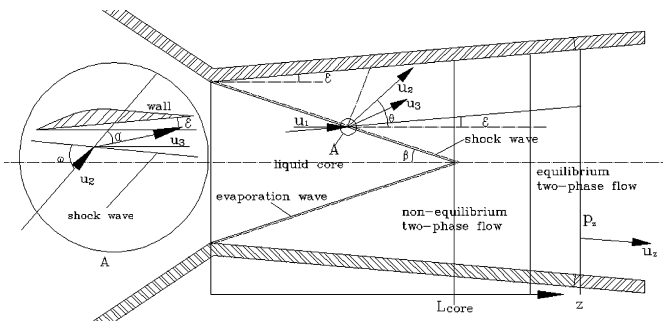

Fig. 3. The shock wave behaviors of fluid in the divergent section.

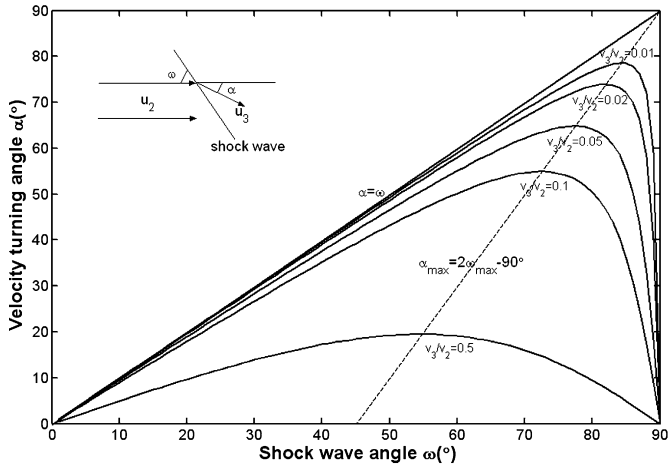

Fig. 4. The relationship between the shock wave angle ω and the velocity turning angle α for several specific volume ratios.

the fluid immediately downstream the shock wave will not flow along the nozzle wall in the divergent section. It can be assume that if the angle between the velocity downstream the evaporation wave (u_2) and the nozzle wall is smaller than the maximal turning angle, the velocity turning angle downstream the shock wave is assumed equal to the angle between the velocity downstream the evaporation wave and the nozzle wall, i.e. the flow is parallel to the nozzle wall. On the contrary, it is equal to the maximal turning angle after the shock wave.

$$\alpha = \begin{cases} \phi & \text{if } \alpha_{\max} > \phi \\ \alpha_{\max} & \text{if } \alpha_{\max} < \phi \end{cases} \tag{29}$$

where, ϕ is the angle between the velocity downstream the evaporation wave (u_2) and the nozzle wall.

Then, the oblique shock wave can be solved.

Combining Eqs. (24), (27) and (28), one can obtain

$$\tan^2\omega = \frac{u_2^2 v_2^2 - 2(h_0 - h_3)v_2^2}{2(h_0 - h_3)v_2^2 - u_2^2 v_3^2} \tag{30}$$

Combining Eqs. (25), (26) and (30), one can obtain

$$p_3 - p_2 = \frac{u_2^2 - 2(h_0 - h_3)}{v_2 + v_3} \tag{31}$$

Then

$$x_3 = \frac{2(h_0 - h_{l3}) + (p_3 - p_2)(v_2 + v_{l3}) - u_2^2}{2(h_{g3} - h_{l3}) - (p_3 - p_2)(v_{g3} - v_{l3})} \tag{32}$$

Eq. (32) has two variables which are p_3 and x_3 respectively. Together with Eq. (29), the state immediately downstream the oblique shock wave can be obtained.

2.5. The pressure profile in divergent section

After the shock wave, the fluid must undergo a sudden condensing process in which the fluid must deviate from homogeneous equilibrium, i.e. non-homogeneous equilibrium state must appear for a distance downstream the throat. To the authors' knowledge, owing to the complexity of the non-homogeneous equilibrium region, no model can sufficiently analyze it, so does the current model in this paper. Because it is the fluid state at the nozzle exit that one is usually interested in, the pressure in the non-homogeneous equilibrium region downstream the throat is not investigated in this paper and it is assumed to be equal to the pressure immediately downstream the shock wave in this region. So the pressure profile in this section must be distinctively deviated from the experimental results.

The behavior downstream the non-homogeneous region in the divergent section is the focus of our attention. It is assumed that the fluid expansion downstream the shock wave is in Isentropic Homogeneous Equilibrium (IHE).

$$s = s_3 = \text{constant} \tag{33}$$

From the mass and energy conservation laws, one can obtain

$$m_0 = \frac{u_z \cos\varepsilon A_z}{v_z} \tag{34}$$

$$h_z = h_0 - \frac{1}{2}u_z^2 \tag{35}$$

Solving Eqs. (33), (34) and (35), one can get the pressure profile downstream the non-homogeneous region in the divergent section.

3. Results and discussion

3.1. Oblique evaporation wave

The pressures and the velocities immediately upstream and downstream the evaporation wave varying with the inlet stagnation conditions are shown in Figs. 5 and 6. The pressures are all increased as the inlet stagnation pressure is increased. The velocity immediately upstream the evaporation wave is also increased, and the velocity immediately downstream the evaporation wave is slightly decreased first, and then, is increased, as the inlet stagnation pressure is increased. There are pressure and velocity jumps after the superheated liquid undergoes an oblique evaporation wave. The pressure difference between p_1 and p_2 is also increased as the inlet stagnation pressure is

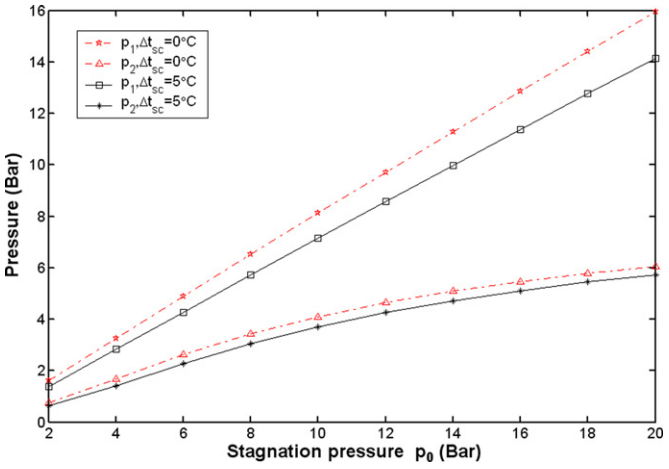

Fig. 5. The pressures immediately upstream the evaporation wave p_1 and downstream the evaporation wave p_2 varying with the inlet stagnation conditions.

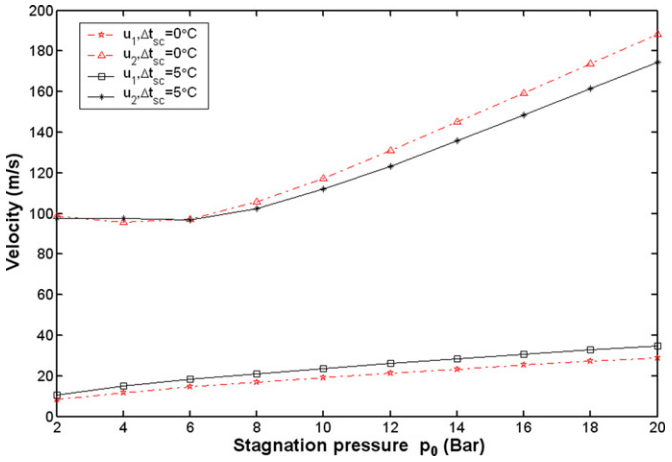

Fig. 6. The velocities immediately upstream the evaporation wave u_1 and downstream the evaporation wave u_2 varying with the inlet stagnation conditions.

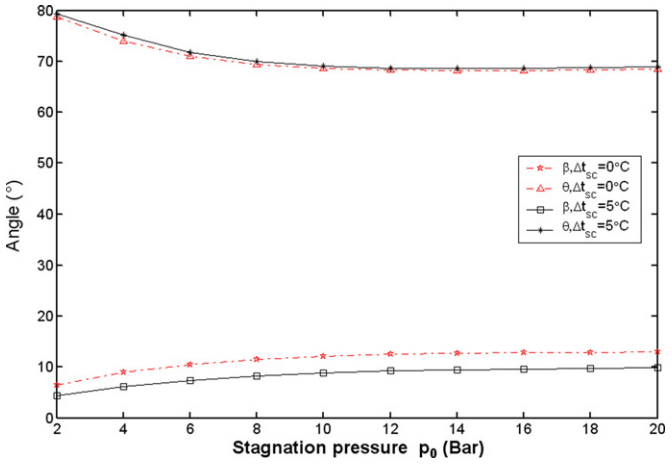

Fig. 7. The velocity turning angle θ and the evaporation wave angle β varying with the inlet stagnation conditions.

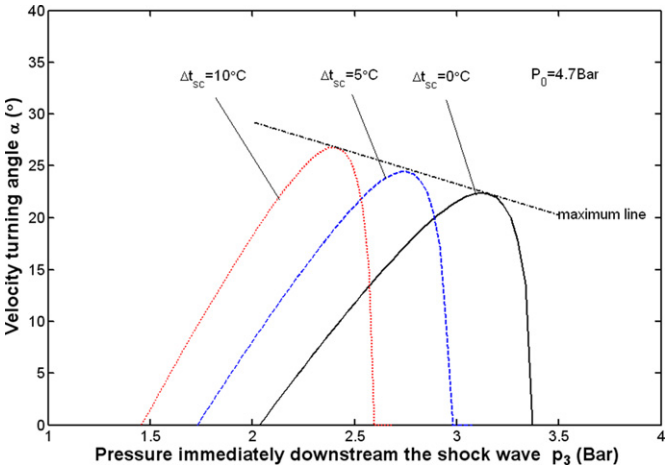

Fig. 8. Velocity turning angle varying with the pressure immediately downstream the shock wave.

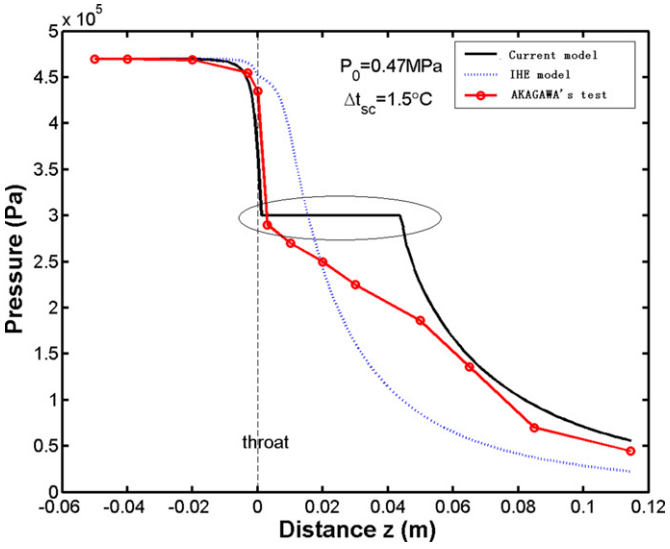

Fig. 9. Comparison between the pressure profiles calculated by the model and the tested result of Akagawa [23].

increased. With the increasing initial inlet subcooled degree, the pressures upstream and downstream the oblique evaporation wave are all decreased. With the increasing initial inlet subcooled degree, the velocity upstream the oblique evaporation wave is increased and the velocity downstream the oblique evaporation wave is decreased.

The velocity turning angle θ and the evaporation wave angle β varying with the inlet stagnation conditions are shown in Fig. 7. One can see that the velocity turning angle θ is extremely larger than the evaporation wave angle, which is analogous to the flashing jet into a big space [22]. It means that the fluid immediately downstream the evaporation wave does not flow along the nozzle wall and shock wave must occur downstream the evaporation wave. With the increasing inlet subcooled degree, the evaporation wave angle is decreased and the velocity turning angle is increased.

3.2. Pressure profile

The velocity turning angle varying with the pressure immediately downstream the shock wave is shown in Fig. 8. The velocity turning angle is increased first, then is decreased, as the pressure immediately downstream the shock wave is increased. There is a maximal velocity turning angle after shock wave. As the inlet subcooled degree is increased, the maximal velocity turning angle is increased and the corresponding pressure immediately downstream the shock wave is decreased.

The comparison between the pressure profiles calculated by current model and the tested result of Akagawa [23] is shown in Fig. 9. The pressure profile upstream the throat is nearly overlapped with the tested result of Akagawa, which validates the mass flux calculated by Abuaf's model. The pressure at the throat calculated by current model is very close to Akagawa's experimental value, about 4% deviation from it, which validates the above stated behaviors immediately downstream the throat. The pressure profile at the back of the divergent section agrees very well with Akagawa's experimental result. The pressure at the exit calculated by the current model is about 10% higher than that tested by Akagawa. The reason for this may be that friction influence is neglected in current model. Since fluid downstream the shock wave near the throat in the divergent sec-

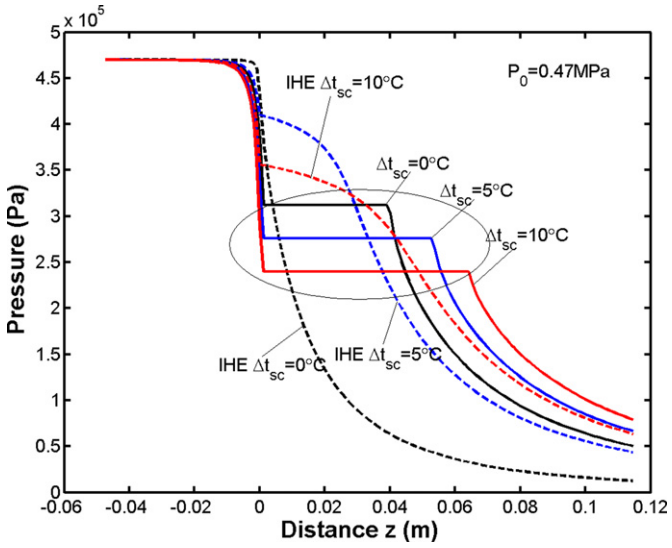

Fig. 10. Comparison between the pressure profiles calculated by current model and calculated by IHE model.

tion is in non-homogeneous equilibrium (marked with ellipse in Figs. 9 and 10), its behaviors are not investigated in this paper, and the pressure at this section is assumed to be equal to the pressure immediately downstream the shock wave. Therefore, it distinctively deviates from Akagawa's tested result.

The comparison of the pressure profiles calculated by current model for different inlet subcooled degrees is shown in Fig. 10. In order to explicitly illustrate the fluid behaviors, the pressure profile calculated by IHE (Isentropic Homogeneous Equilibrium) model is also shown in this figure. Compared with the IHE model, there is a sudden pressure jump at the throat which is resulted by the evaporation wave. The pressure at the nozzle exit is higher than that calculated by IHE model, which means that the velocity at the nozzle exit is lower than that calculated by IHE model. This is because some available energy is lost owing to the evaporation wave and the shock wave in the divergent section. As the inlet subcooled degree is increased, the pressure at the throat is decreased, but the pressure in the homogeneous region in the divergent section is increased, which means that the exit velocity gets lower. The length of the non-homogeneous equilibrium region is increased as the initially inlet subcooled degree is increased. Therefore, in order to obtain higher velocity at the convergent–divergent nozzle exit, the length of the divergent section should be increased as the inlet subcooled degree is increased.

4. Conclusion

The flashing flow behaviors of initially subcooled liquid when it flows in convergent–divergent nozzles are investigated in this paper. It is found that not only evaporation wave but also shock wave occurs in nozzles, and non-homogeneous equilibrium region exists near the throat in the divergent section.

A model, in which the oblique evaporation wave theory and the oblique shock wave theory are employed, is developed to investigate the performance of convergent–divergent nozzles. Numerical analysis is carried out. The results show that the pressure at the throat is very close to the experimental result, about 4% deviation from Akagawa's tested value. Owing to the evaporation wave and the shock wave, the exit velocity is lower than that calculated by IHE model. The length of the non-homogeneous equilibrium region in the divergent section is increased as the initially inlet subcooled degree is increased. The pressure profile predicted by the model agrees very well with the tested profile of Akagawa except in the non-homogeneous equilibrium region near the throat in the divergent section.

References

[1] P.A. Thompson, G.C. Carofano, Y.G. Kim, Shock waves and phase changes in a large-heat-capacity fluid emerging from a tube, Journal of Fluid Mechanics 166 (1986) 57–92.
[2] P.A. Thompson, H. Chaves, G.E.A. Meier, Y.G. Kim, H.D. Speckman, Wave splitting in a fluid of large heat capacity, Journal of Fluid Mechanics 185 (1987) 385–414.
[3] M.D. Alamgir, J.H. Lienhard, Correlation of pressure undershoot during hot water depressurization, ASME Journal of Heat Transfer 103 (1981) 52–55.
[4] O.C. Jones Jr., Flashing inception in flowing liquid, ASME Journal of Heat Transfer 102 (1980) 754–764.
[5] N. Abuaf, O.C. Jones Jr., B.J.C. Wu, Critical flashing flows in nozzles with subcooled inlet conditions, ASME Journal of Heat Transfer 105 (1983) 379–383.
[6] V.E. Schrock, E.S. Starkman, R.A. Brown, Flashing flow of initially subcooled water in convergent–divergent nozzles, ASME Journal of Heat Transfer 99 (1977) 263–268.
[7] P. Reinke, G. Yadigaroglu, Explosive vaporization of superheated liquids by boiling front, International Journal of Multiphase Flow 27 (9) (2001) 1487–1516.
[8] J.R. Simoes-Moreira, J.E. Shepherd, Evaporation waves in superheated dodecane, Journal of Fluid Mechanics 382 (1999) 63–86.
[9] J.R. Simoes-Moreira, Oblique evaporation waves, Shock Waves 10 (2000) 229–234.
[10] J.R. Simoes-Moreira, M.M. Vieira, E. Angelo, Highly expanded flashing liquid jets, Journal of Thermophysics and Heat Transfer 16 (3) (2002) 415–424.
[11] J.R. Simoes-Moreira, C.W. Bullard, Pressure drop and flashing mechanisms in refrigerant expansion devices, International Journal of Refrigeration 26 (7) (2003) 840–848.
[12] E.S. Hutmacher, B.J. Nesmith, J.B. Brukiewa, Study of safety relief valve operation under ATWS condition, Energy Technology Engineering Center, ETEC-TDR-78-19, Jan. 1979.
[13] Y.Y. Hsu, Review of critical flow, propagation of pressure pulse and sonic velocity, NASA TND-6814, 1972.
[14] P. Saha, Review of two-phase steam–water critical flow models with emphasis on thermal nonequilibrium, NUREG/CR 0417, BNL-NUREG-50907, 1978.
[15] H.S. Isbin, Some observations on the status of two-phase critical flow model, International Journal of Multiphase Flow 6 (1980) 131–137.
[16] E. Elias, P.L. Chambre, A mechanic non-equilibrium model for two-phase critical flow, International Journal of Multiphase Flow 10 (1) (1984) 21–40.
[17] H.J. Richter, Separated two-phase flow model: Application to critical two-phase flow, International Journal of Multiphase Flow 9 (5) (1983) 511–530.
[18] K.H. Ardron, A two-fluid model for critical vapour–liquid flow, International Journal of Multi-phase Flow 4 (1978) 323–337.
[19] T.S. Shin, O.C. Jones, Nucleation and flashing in nozzles—1: A distributed nucleation model, International Journal of Multiphase Flow 19 (6) (1993) 943–964.
[20] V.N. Blinkov, O.C. Jones, B.I. Nigmatulin, Nucleation and flashing in Nozzles—2: Comparison with experiments using a five-equation

model for vapor void development, International Journal of Multiphase Flow 19 (6) (1993) 965–986.
[21] G.A. Pinhasi, A. Dayan, A. Ullmann, Modeling of flashing two-phase flow, Reviews in Chemical Engineering 21 (3–4) (2005) 133–264.
[22] R.E. Athans, The rapid expansion of near-critical retrograde fluid, PhD thesis, Rensselaer Polytechnic Institute, New York, 1995.
[23] K. Akagawa, T. Fuji, J. Ohta, K. Inoue, K. Taniguchi, Performance characteristics of divergent–convergent nozzles for subcooled hot water, JSME International Journal, Series II 31 (4) (1988) 718–726.